

## Preparation of Carbon-supported Pt–Co Alloy Nanoparticles for Oxygen Reduction Reaction: Promotion of Pt–Co Alloy Formation by Coverage with Silica

Sakae Takenaka,\* Akiko Hirata, Hideki Matsune, and Masahiro Kishida  
 Department of Chemical Engineering, Graduate School of Engineering, Kyushu University,  
 744 Moto-oka, Nishi-ku, Fukuoka 819-0395

(Received February 23, 2010; CL-100178; E-mail: takenaka@chem-eng.kyushu-u.ac.jp)

Carbon-supported Pt–Co catalyst for the oxygen reduction reaction was covered with silica layers to inhibit sintering of the metal particles. Coverage of the Pt–Co catalyst with silica layers promoted the formation of alloys with small diameters during treatment at 973 K. The silica-coated Pt–Co electrocatalyst showed a large electrochemically active surface area (ECSA) and excellent durability.

The insufficient catalytic activity and low stability of Pt catalysts for the oxygen reduction reaction (ORR) at the cathode in polymer electrolyte fuel cells (PEFCs) impede the full commercialization of PEFCs. Many research groups have developed Pt-based alloy catalysts with high activity and excellent durability for the ORR. Pt–Co alloys have been extensively studied as Pt-based alloy catalysts.<sup>1</sup> The loading of Pt in the catalyst at the cathode can be reduced when Pt–Co alloy catalysts are used in PEFCs since the catalytic activity of the Pt–Co alloy for the ORR, based on Pt mass, is higher than that of pure Pt. Bimetallic catalysts have been used in many catalytic reactions in addition to PEFCs.<sup>2</sup> Generally, bimetallic catalysts are treated at high temperatures to form alloys. The treatment of the catalysts at high temperatures improves the degree of alloying, but the alloy particles aggregate easily to form larger diameter particles. Therefore, the aggregation of alloy particles during treatment at high temperatures should be suppressed.

We have previously studied metal nanoparticle catalysts such as Pt and Ni covered with silica.<sup>3</sup> Metal particles within silica-coated catalysts showed high durability to sintering at high temperatures because these metal particles were not in direct contact with other particles. In addition, we have demonstrated that carbon-supported Pt catalysts covered with silica layers showed high activity and excellent durability in the ORR of PEFCs.<sup>4</sup> We expect that the coverage of Pt–Co supported on carbon with silica will promote the formation of a small particle size Pt–Co alloy. In this study, carbon-supported Pt–Co catalysts were covered with silica to obtain Pt–Co alloys with small particle sizes.

For the preparation of carbon black-supported Pt–Co (Pt–Co/CB),  $\text{H}_2\text{PtCl}_6$  and  $\text{CoCl}_2$  were dissolved in ethylene glycol.<sup>5</sup> After the pH of this solution was adjusted to 13 by the addition of NaOH, carbon black (Vulcan XC-72) was added to the solution and it was refluxed at 443 K for 4 h. After washing and drying, the sample was reduced with  $\text{H}_2$  at 623 K. The Pt–Co/CB obtained was covered with silica by the successive hydrolysis of 3-aminopropyltriethoxysilane (APTES) and tetraethoxysilane (TEOS).<sup>4</sup> The Pt–Co/CB was dispersed in a mixture of water and ethanol. APTES and triethylamine were added to the solution. After mixing the solution at 353 K, TEOS was added to the solution. These Pt–Co samples with or without silica were reduced with  $\text{H}_2$  at 623 K and further treated at 973 K

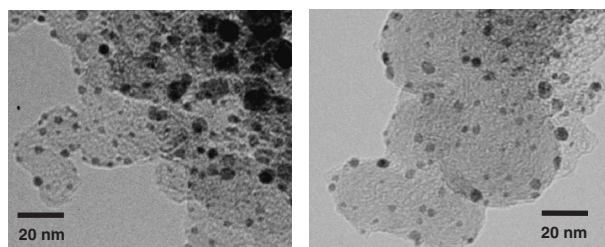


**Figure 1.** TEM images of Pt–Co/CB (left) and  $\text{SiO}_2/\text{Pt-Co/CB}$  (right) after treatment at 973 K.

in Ar to allow alloy formation. The silica-coated Pt–Co catalyst is denoted as  $\text{SiO}_2/\text{Pt-Co/CB}$ .

Cyclic voltammograms (CVs) of the Pt–Co catalysts were measured in  $\text{N}_2$ -purged 0.1 M  $\text{HClO}_4$  using a three compartment electrochemical cell with a Pt mesh and a  $\text{Ag}/\text{AgCl}$  electrode serving as counter and reference electrodes, respectively. All potentials are given relative to the reversible hydrogen electrode (RHE). The Pt–Co catalyst was attached onto a glassy carbon rod (diameter 5 mm) using Nafion. An accelerated durability test for the Pt–Co catalyst was performed using the same cells. The potential of the catalyst was repeatedly changed between 0.05 and 1.0 V at 333 K.<sup>4</sup> ECSA of Pt in the Pt–Co catalyst was evaluated from the desorption of underpotentially deposited hydrogen in the CV of the Pt–Co catalyst.

Figure 1 shows TEM images of Pt–Co/CB and  $\text{SiO}_2/\text{Pt-Co/CB}$ . The loading of Pt and Co in Pt–Co/CB was evaluated using X-ray fluorescence spectroscopy and found to be 8.1 and 2.2 wt %, respectively. The amount of  $\text{SiO}_2$  in  $\text{SiO}_2/\text{Pt-Co/CB}$  was estimated to be 15 wt %. In the TEM image of Pt–Co/CB, metal particles were observed and the particle size was widely distributed from 2 to 10 nm. On the basis of the TEM images for Pt–Co/CB, the average particle size was determined to be 4.8 nm. Many metal particles were also supported on the CB surface as clarified in the TEM image of  $\text{SiO}_2/\text{Pt-Co/CB}$ . However, silica was not found in this TEM image. This is due to the small amount of silica in the catalyst. It should be noted that the particle size of  $\text{SiO}_2/\text{Pt-Co/CB}$  was very uniform and smaller than that of Pt–Co/CB. The average size of metal particles in  $\text{SiO}_2/\text{Pt-Co/CB}$  was 2.6 nm. These catalysts were treated at 973 K in Ar before the measurement of TEM images. The silica layers wrapped around the metal particles in  $\text{SiO}_2/\text{Pt-Co/CB}$  prevented the aggregation of metal particles during treatment at 973 K.

Figure 2 shows XRD patterns of Pt/CB, Pt–Co/CB, and  $\text{SiO}_2/\text{Pt-Co/CB}$ . Peaks due to Pt metal are present at around 39 and 46 degrees in the XRD pattern of Pt/CB. The position of the peaks in the XRD pattern for Pt–Co/CB was very similar to those for Pt/CB. In addition, a peak was also observed at around 44

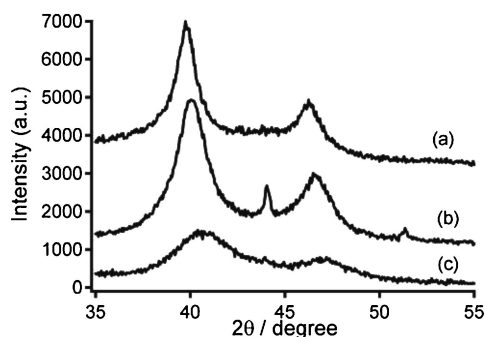


**Figure 2.** XRD patterns of Pt/CB (a), Pt-Co/CB (b), and SiO<sub>2</sub>/Pt-Co/CB (c).

degrees in the XRD pattern of Pt-Co/CB. This peak would be due to Co metal or Pt-Co alloys with a high Co/Pt mole ratio. Thus, the degree of alloying for Pt-Co/CB was low. In contrast, a peak at around 40 degrees in the XRD pattern of SiO<sub>2</sub>/Pt-Co/CB shifted to higher angles compared with that in Pt-Co/CB and no peak at 44 degrees was present, indicating that the alloying degree for SiO<sub>2</sub>/Pt-Co/CB was higher than that of Pt-Co/CB. In addition, the peaks due to metals in the XRD pattern of SiO<sub>2</sub>/Pt-Co/CB were broader than those for Pt-Co/CB. Therefore, the metal particles in SiO<sub>2</sub>/Pt-Co/CB were present as a Pt-Co alloy with small crystallite sizes. The coverage of Pt-Co/CB with silica layers promotes alloy formation between Pt and Co.

Figure 3 shows CVs of Pt-Co/CB and SiO<sub>2</sub>/Pt-Co/CB in N<sub>2</sub>-purged HClO<sub>4</sub> during potential cycling experiments. In the CV of fresh Pt-Co/CB, two peak couples were present and were due to the adsorption and desorption of hydrogen on the surface of Pt from 0.05 to 0.3 V and the oxidation and reduction of Pt from 0.6 to 1.20 V. The ECSA of Pt for fresh Pt-Co/CB was estimated to be 64 m<sup>2</sup> g-Pt<sup>-1</sup> from the CV. These peaks were also present in the CV of fresh SiO<sub>2</sub>/Pt-Co/CB indicating that the catalyst is electrochemically active despite the coverage of Pt-Co alloys with the silica insulator. Reactant molecules such as water and protons diffuse into the Pt-Co alloy surface through porous silica layers, and electrons conduct into the alloys through exposed CB surfaces. Therefore, SiO<sub>2</sub>/Pt-Co/CB shows electrocatalytic activity. The ECSA of fresh SiO<sub>2</sub>/Pt-Co/CB was 60 m<sup>2</sup> g-Pt<sup>-1</sup>, which was slightly smaller than that of fresh Pt-Co/CB. Some Pt-Co alloy particles in SiO<sub>2</sub>/Pt-Co/CB may be electrochemically inactive because of coverage with thick silica layers. The peaks due to Pt in the CVs of Pt-Co/CB gradually decreased in intensity during potential cycling. The ECSAs for Pt-Co/CB decreased from 64 to 30 m<sup>2</sup> g-Pt<sup>-1</sup> after 6000 cycles of potential cycling. In contrast, the peak intensity in the CVs of SiO<sub>2</sub>/Pt-Co/CB did not change during potential cycling. The ECSA of SiO<sub>2</sub>/Pt-Co/CB after 6000 cycles was 50 m<sup>2</sup> g-Pt<sup>-1</sup>. Figure 4 shows TEM images of Pt-Co/CB and SiO<sub>2</sub>/Pt-Co/CB after 6000 cycles of potential cycling. The size of metal particles in used Pt-Co/CB ranged from 4 to 20 nm, and the average particle size was 7.2 nm. This was significantly larger than that for fresh Pt-Co/CB. In contrast, the size of the Pt-Co alloy in SiO<sub>2</sub>/Pt-Co/CB did not change appreciably after 6000 cycles. The average particle size of Pt-Co alloy in used SiO<sub>2</sub>/Pt-Co/CB was 3.4 nm. From these results, we conclude that SiO<sub>2</sub>/Pt-Co/CB shows excellent durability for electrochemical reactions in acid electrolytes. The higher degree of alloying in Pt-Co and

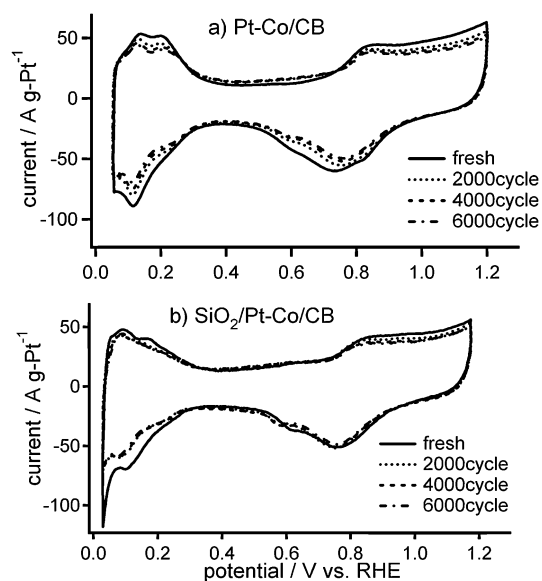


**Figure 3.** CVs of Pt-Co/CB (a) and SiO<sub>2</sub>/Pt-Co/CB (b) in N<sub>2</sub>-purged HClO<sub>4</sub> at 333 K during potential cycling.

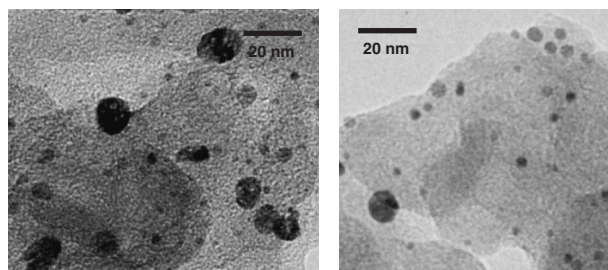


**Figure 4.** TEM images of used Pt-Co/CB (left) and SiO<sub>2</sub>/Pt-Co/CB (right).

the coverage of alloy particles with silica layers resulted in the high durability of SiO<sub>2</sub>/Pt-Co/CB.<sup>4,6</sup>

In conclusion, the coverage of Pt-Co catalysts with silica layers improves the degree of alloying for smaller sized Pt-Co particles. Silica-coated Pt-based alloy catalysts have large ECSAs and excellent durability. Therefore, the silica-coating technique is useful for the preparation of various alloy nanoparticle catalysts.

This work was supported by a Grand-in-Aid of Scientific Research B (No. 20360365) from the Ministry of Education, Culture, Sports, Science and Technology of Japan.

#### References

- 1 M. Watanabe, K. Tsurumi, T. Mizukami, T. Nakamura, P. Stonehart, *J. Electrochem. Soc.* **1994**, *141*, 2659.
- 2 K. Yoshida, N. Begum, S. Ito, K. Tomishige, *Appl. Catal., A* **2009**, *358*, 186; G. Wang, T. Takeguchi, E. N. Muhamad, T. Yamanaka, M. Sadakane, W. Ueda, *J. Electrochem. Soc.* **2009**, *156*, B1348; S. Takenaka, Y. Shigeta, E. Tanabe, K. Otsuka, *J. Phys. Chem. B* **2004**, *108*, 7656.
- 3 S. Takenaka, H. Umebayashi, E. Tanabe, H. Matsune, M. Kishida, *J. Catal.* **2007**, *245*, 392.
- 4 S. Takenaka, H. Matsumori, K. Nakagawa, H. Matsune, E. Tanabe, M. Kishida, *J. Phys. Chem. C* **2007**, *111*, 15133.
- 5 J. Shen, Y. Hu, C. Li, C. Qin, M. Ye, *Electrochim. Acta* **2008**, *53*, 7276.
- 6 H. R. Colón-Mercado, B. N. Popov, *J. Power Sources* **2006**, *155*, 253.